FRICTION AND WEAR RESPONSE OF TiB_2-B_4C CERAMICS

Y. Pérez Delgado[1], K. Bonny[1], P. De Baets[1], M. H. Staia[2], P. D. Neis[3], N. F. Ferreira[3], O. Malek[4,5], J. Vleugels[4], B. Lauwers[5]

[1] Department of Mechanical Construction and Production, Laboratory Soete, Ghent University
[2] School of Metallurgical Engineering and Materials Science, Universidad Central de Venezuela
[3] Federal University of Rio Grande do Sul, Porto Alegre, Brazil
[4] Metallurgy and Materials Engineering Department, Catholic University of Leuven, Belgium
[5] Mechanical Engineering Department, Catholic University of Leuven University, Belgium

Abstract: Rotating sliding wear experiments on TiB_2-B_4C have been conducted at room temperature (25 °C) in dry conditions according to the ASTMG99-95a standard. SiC balls were used as static counterpart. The disk specimens were surface finished by polishing. The tests were performed using different rotating sliding speeds from 0.1 up to 1.5 m/s with a mean Hertzian contact pressure of 1.2 GPa. Balls and disk specimens were analyzed by 2-D and 3-D surface topography, SEM and optical microscopy. The experimental results demonstrated that the sliding velocity influences both friction coefficient and wear rate values of TiB_2-B_4C ceramics. It was shown, that the wear rate varied between 3.64E-7 to 8.43E-7 mm^3/Nm. Wear mechanisms such as polishing, abrasion and wear debris formation have been identified by means of SEM and EDX technique.

Keywords: TiB_2-B_4C; friction; wear rate; room temperature; ball-on-disk; wear mechanisms

1 INTRODUCTION

Monolithic B_4C is well known for its exceptional properties such as high melting point (~ 2450 °C), low density, chemical stability and extreme hardness (just behind of diamond and cubic-BN). B_4C has an industrial significance and has been used in lightweight armour plates; nuclear applications due to its neutron absorption; electrical application (boron carbide/graphite thermocouple) and wear applications such abrasion media, grinding wheels, water-jet nozzles, etc. Nevertheless, it is also known that monolithic B_4C has some particular drawbacks such as poor sinterability, limited strength and fracture toughness [1].

Several attempts to promote densification at relative low temperature have been already done by adding different sintering additives such as e.g. TiB_2, TiB_2+C, W_2B_5, B +C, B + Si, Si, Al, Mg, Ni, SiC [1-5].

The TiB_2 phase serves as a sintering aid significantly improving densification, mechanical properties (strength and fracture toughness) by means of the grain refiner and diffusion effect [6]. Besides improving the sinterability and mechanical properties, the addition of TiB_2 electrically conductive particles on the she semi-conductor B_4C matrix, allows the implementation of electrical discharge machining (EDM) of the ceramic composite.

In the present paper, TiB_2-B_4C composite was made by means of pulsed electric current sintering (PECS) or also called spark plasma sintering (SPS). This sintering technique has the advantage of higher heating rates and shorter dwell times in comparison with conventional methods (pressureless and hot pressing).

Independently, monolithic TiB_2 and B_4C have been already used for wear applications [1, 3]. TiB_2-B_4C ceramic composite might also be a good candidate for such applications. A problem, however, is the lack of knowledge of wear response of PECS TiB_2-B_4C ceramics composite.

This paper aims at evaluating and comparing the friction and wear response of PECS TiB_2-B_4C ceramic composite in rotating sliding contact, and examines how the tribological characteristics are affected by the interaction of wear particles and sliding speed.

2 EXPERIMENTAL

2.1 Material properties

TiB_2-B_4C (B_4C 40 %vol) ceramic was fully densified without any additives by means of pulsed electric current sintering (PECS). Further information on the processing can be found elsewhere [5]. The test

specimens display a Vickers hardness $HV_{,1kg}$ of 2945 ± 30 kg/mm^2, an E-modulus of 537 ± 3.5 GPa, a flexural strength of 867 ± 131 MPa, a fracture toughness $K_{IC,1kg}$ of 4.5 ± 0.1 MPa.m$^{1/2}$, a density of 3.72 g/cm^3, a thermal conductivity of 68.27 W/m.°K [7] and a specific heat of 704.2 J/(kg.°K) according to the rule of mixture using 940 J/(kg. °K) and 617 J/(kg. °K) for B_4C and TiB_2, respectively.

The Vickers hardness was measured with indentation load of 9.81 N for 15 s (Model FV-700, Future-Tech Corp., Tokyo, Japan). The Young's modulus, E, was obtained by resonance frequency method (ASTM C 1259-94) on a Grindo-sonic (J.W. Lemmens, Elektronika N.V., Leuven, Belgium). The flexural strength was measured on a 3-point bending test set-up (INSTRON 4467, Instron Corp., USA) with a span of 20 mm. The fracture toughness, $KIC_{,1kg}$ was obtained by Vickers indentation according to Anstis *et al.* [8].

The TiB_2-B_4C specimens were ground with a diamond-grinding wheel (type D46SW-50-X2, Technodiamant, The Netherlands) on a Jung grinding machine (JF415DS, Jung, Germany). The polished surface finish was obtained subsequent to the grinding process using two consecutive polishing steps using diamond paste of 9 µm and 3 µm, respectively. After grinding and polishing the disk specimens had a thickness of approximately 4 mm and a diameter of 40 mm.

The surface roughness of the TiB_2-B_4C composite ceramic was measured using surface profilometry (Somicronic® EMS Surfascan 3D, type SM3, needle type ST305) according to the ISO 4228 standard. The roughness equalled Ra = 0.020 ± 0.002 µm and Rt = 0.140 ± 0.036 µm.

2.2 Tribological characterisation

Wear experiments were conducted on a pin-on disk tribometer (CSM Switzerland) under the configuration of ball on disk (point contact). The tests were carried out according to the ASTM G99-95a standard at room temperature and atmospheric conditions. An initial mean Hertzian pressure of 1.2 GPa was applied with 1 N of normal load. Five different sliding speeds of 0.1, 0.3, 0.5, 1.0 and 1.5 m/s were used. A total sliding distance of 3000 m was run for all the experiments.

The static counterpart was a SiC ball with a diameter of 5 mm and surface roughness Ra 0.025 µm. The SiC ball displays a Vickers hardness of $HV_{,1kg}$ of 2810 kg/mm^2, E-modulus of 410 GPa, flexural strength of 400 MPa, fracture toughness $K_{IC,1kg}$ of 2.7 MPa.m$^{1/2}$ and a density of 3.1 g/cm^3 (specifications given by the supplier) and thermal conductivity of 110 W/m.°K , according to Pasaribu *et al.* [9].

Post-mortem analysis of the disks and SiC balls were conducted by means of two independent techniques: 2D surface topography and optical microscopy, which allowed calculating the specific wear rate k (mm^3/N.m).

3 RESULTS AND DISCUSSION

3.1 Friction coefficients and wear rate

The variation of the friction coefficient with the sliding distance is reported in Figure 1 only or the lowest and highest linear sliding speed of 0.1 and 1.5 m/s, respectively. However, the friction coefficient values for all the 5 different sliding speeds are further summarized in Table 1. The friction coefficient value for all the curves exhibits a sharp increase throughout the first meters of sliding and, subsequently, evolves towards a steady state. Nevertheless, some fluctuations are still evidenced and these are attributed to the formation of wear debris particles and to continuous breaking and interlocking of the sharp particles at the contact surface during sliding. The higher value of the friction coefficient was encountered for the lowest sliding speed of 0.1 m/s, which was related to the small centrifugal force action during the wear test, thus allowing the clustering of particles into the contact area. In fact, as the sliding speed increases to 1.5 m/s, it is expected that these wear debris will be ejected away from the contact which, together with the frictional heating phenomenon that takes place, will lead to a decrease in the value of the friction coefficient.

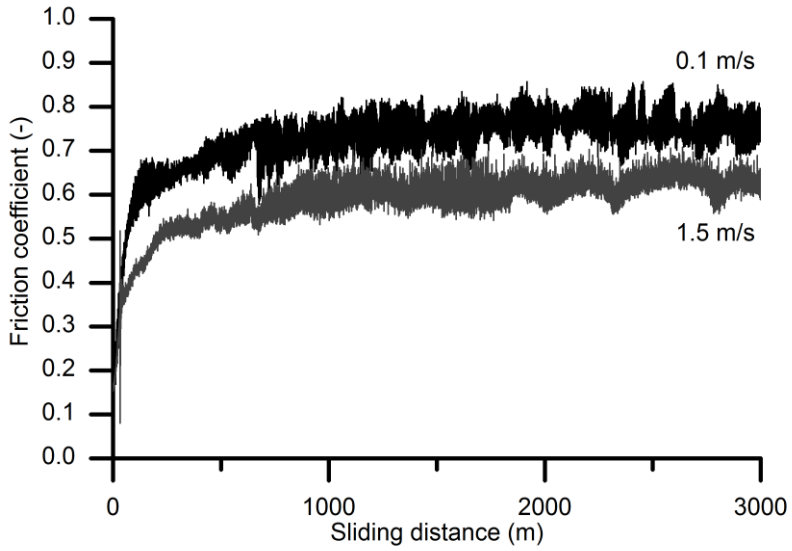

Figure 1. Variation on friction coefficient with the sliding distance; normal load 1 N, sliding distance 3000 m.

The influence of sliding linear speed on the tribological behaviour of TiB_2-B_4C is summarized in both Table 1 and Figure 1, which compare the value for the coefficients of friction, wear volumes and the specific wear rate determined for the experimental settings described above. The coefficient of friction value in this table corresponds to the average value obtained for the last 2000 m sliding distance, i.e. for the distance where the system achieved steady state.

Wear volumes can be extracted from the generated worn tracks by means of the 2D profile section and multiplied by the periphery of the radius under study. The specific wear rate k was obtained from the ratio between wear volume and the applied load per unit of sliding distance. Each value is an average of at least 3 wear experiments performed under identical conditions, with standard deviations of less than 10 % and 15 % for coefficient of friction and specific wear rate, respectively.

Table 1. Variation of friction coefficient, wear rate and wear volume of TiB_2-B_4C ceramics disks with a Hertzian contact pressure of 1.2 GPa.

Speed [m/s]	**μ [-]**	**k_{disk} [mm^3/Nm]**	**V_{disk} [mm^3]**
0.1	0.75	3.6E-07	1.1E-03
0.3	0.67	4.9E-07	1.5E-03
0.5	0.72	6.0E-07	1.8E-03
1.0	0.68	5.2E-07	1.6E-03
1.5	0.62	8.4E-07	2.5E-03

As it could be observed, the dynamic coefficient of friction value decreases almost with 20 % when the sliding speed increases from 0.1 m/s to 1.5 m/s. Meanwhile the specific wear rate has shown an opposite behaviour. It was found that the value of the specific wear rate is of approximately 2.5 times higher when compared to the value obtained for the test carried out at the lowest sliding speed of 0.1 m/s.

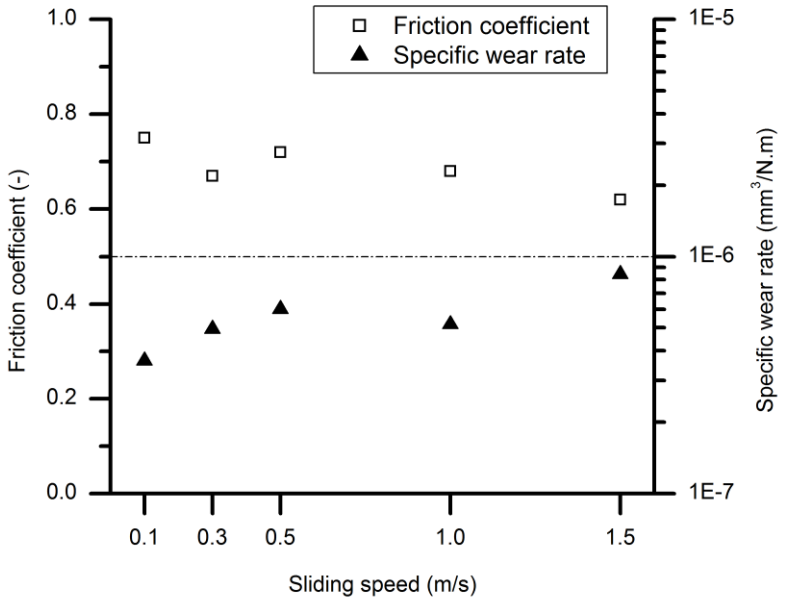

Figure 2. Variation of the friction coefficient and specific wear rate as a function of sliding speed; normal load 1 N, sliding distance 3000 m.

According to Metselaar *et al.* [10] the wear of ceramics under dry sliding conditions is, besides its mechanical overloading, often governed by frictional heating. As it has been already explained by other researchers [9-11] when sliding contact passes a spot, the temperature will raise due to frictional heating and, subsequently, due to heat dissipation, a rapid cooling will induce thermal strain and, therefore, stress at the surface. Bos [12] derived the maximum temperature rise due to frictional heating:

$$\Delta T = \frac{\mu N v}{a K_{eff}} \tag{1}$$

K_{eff} is the effective thermal conductivity [9, 10, 12] that can be calculated as follows:

$$K_{eff} = 2.667\left(K_{stat} + \sqrt{K^2{}_{mov} + 0.4 V a \rho_{mov} c_{mov} K_{mov}}\right) \tag{2}$$

The thermal stress reaches a maximum value, which could be expressed as [11]:

$$\sigma_{max(therm)} = \frac{E\alpha}{1-\nu}\Delta T \tag{3}$$

The maximum stresses due to the frictional heating were calculated by means of the equations described above, using the results obtained in the wear experiments (see Table 2). Moreover, this indicates the relation between $\sigma_{max(therm)}/\mu$ is proportional to the sliding velocity. What is interesting from Table 2 is the fact that the stress at the contact surface due to the frictional heating, $\sigma_{max(therm)}$, at a sliding speed of 1.5 m/s is considerably much higher, approximately 12 times higher, than the value corresponding to the 0.1 m/s, indicating that the test parameter 'sliding speed' does have an important effect on the wear performance.

Table 2. Stresses induced at contact as a consequence of frictional heating.

Speed [m/s]	**0.1**	**0.3**	**0.5**	**1.0**	**1.5**
$\sigma_{max\ (therm\ )}$ [MPa]	29.26	78.41	140.44	265.28	362.81

3.2 Worn surfaces

Post-mortem analysis, for both TiB_2-B_4C disks and SiC balls, were carried out by means of SEM and optical microscopy. A typical wear scar in the disk is shown as well as a worn cap for the SiC ball in Figure 3.

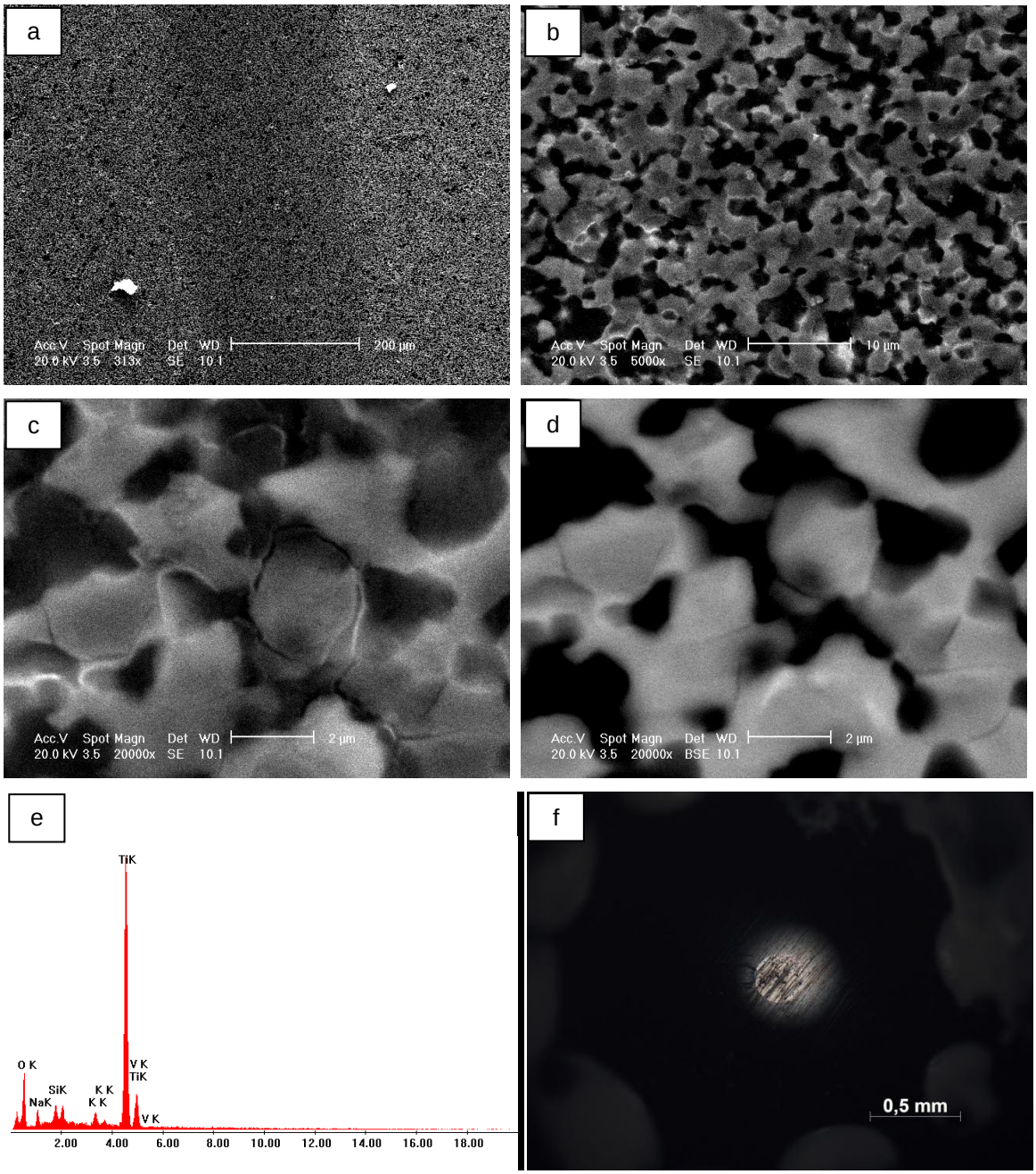

Figure 3. Wear track of TiB_2-B_4C against SiC ball, normal load 1 N, and sliding distance 3000 m: (a) general view; (b) a zoom of (a); (c) typical example of micro-cracks using secondary electrons SE, (d) back-scattered electron detector BSE; (e) EDX analysis and optical microscopy of the SiC ball.

Visual inspections of worn surfaces after wear testing revealed the occurrence of wear debris particles, mainly located in the outer extensions of the wear track, but also occasionally inside, along and adjacent to the wear scar.

SEM images (Figures 3a and 3b) of the worn surface on the disk indicate a polished smooth surface with some abrasion scratch marks. Furthermore, the occurrence of micro-cracks in the surface is also observed (Figure 3c). This could be explained in terms of the thermal impact of the frictional heating, previously expressed in Eq. (3) which combined with the mechanical impact, as consequence of the normal and friction force in the contact, will intensify the induced tensile stress at trailing edge of the contact [13].

This maximum tensile stress is given by

$$\sigma_{max\ (mec\ )} = \frac{3N}{2\pi a^2}\left[\frac{1-2\nu}{3} + \frac{4+\nu}{8}\pi\mu\right] \quad (4)$$

Additionally, elementary chemical analysis by EDX and Back-Scattered Electron Detector (BSE) were used. The bright grey and black contrast grains in the BSE image (Figure 3d) are TiB_2 and B_4C respectively. Moreover, traces of silicon, which comes from the SiC ball, were observed in the worn track (Figure 3e), putting in evidence the presence and interaction of the wear debris on the sliding contact. The worn cap of the SiC ball was investigated by optical microscopy (Figure 3f) showing just some polishing and abrasion patterns. It is worth noting that similar wear mechanisms were determined for all the samples tested in the present research.

4 CONCLUSIONS

Rotating wear experiments on TiB_2-B_4C slid against SiC balls revealed that the sliding speed has a significant effect on the wear performance. The friction coefficient was encountered to decrease up to approximately 20 % when the sliding speed increases to 1.5 m/s, which can be attributed to the less interaction of wear debris particles on the contact, compared to the one obtained at 0.1 m/s. On the contrary, the specific wear rate increases with the sliding speed and values varying from 3.6E-07 until 8.4E-07 mm^3/Nm were determined, thus indicating that wear of ceramics under dry sliding conditions is, besides mechanical overloading, often governed by frictional heating. Wear mechanisms such as polishing, abrasion and wear debris formation have been identified on the disk as well as on the ball by means of SEM, EDX and optical microscopy.

5 NOMENCLATURE

μ	Friction coefficient	-
k_{disk}	Specific wear rate of disk	mm^3/N m
N	Normal load	N
v	Sliding speed	m/s
a	Hertzian contact area	mm^2
K_{eff}	Effective thermal conductivity	W/m °K
K_{stact}	Thermal conductivity of ball	W/m °K
K_{mov}	Thermal conductivity of disk	W/m °K
ρ_{mov}	density	kg/m^3
c_{mov}	Specific heat	J/kg °K
α	Thermal expansion coefficient	$x10^{-6}$ $°K^{-1}$
E	Young's modulus	GPa
υ	Poisson ratio	-
$\sigma_{max(therm)}$	Tensile stress induced by thermal strain	GPa
$\sigma_{max(mech)}$	Tensile stress induced by mechanical contact	GPa

6 ACKNOWLEDGEMENTS

The authors would like to acknowledge the support of the Fund for Scientific Research Flanders (FWO, Grant No. G.0539.08) and the Flemish Institute for the promotion of Innovation by Science and Technology in industry (IWT, Grant No. GBOU-IWT-010071-SPARK). Professor M. Staia gratefully acknowledges the financial support from Ghent University (BOF).

7 REFERENCES

1. Thévenot, F., *Boron carbide—a comprehensive review.* Journal of the European Ceramic Society, 1990. **6**(4): p. 205-225.

2. Patel, M., et al., *Processing and characterization of B< sub> 4</sub> C–SiC–Si–TiB< sub> 2</sub> composites.* Materials Science and Engineering: A, 2010. **527**(16): p. 4109-4112.
3. Munro, R.G., *Material properties of titanium diboride.* Journal of Research of the National Institute of Standards and Technology, 2000. **105**(5): p. 709-720.
4. Sigl, L., *Processing and mechanical properties of boron carbide sintered with TiC.* Journal of the European Ceramic Society, 1998. **18**(11): p. 1521-1529.
5. Huang, S.G., et al., *Microstructure and mechanical properties of pulsed electric current sintered B4C–TiB2 composites.* Materials Science and Engineering: A, 2011. **528**(3): p. 1302-1309.
6. Skorokhod, V., *Processing, Microstructure, and Mechanical Properties of B4C — TiB2 Particulate Sintered Composites. Part I. Pressureless Sintering and Microstructure Evolution.* Powder Metallurgy and Metal Ceramics, 2000. **39**(7-8): p. 414-423.
7. Malek, O., et al., *Electrical discharge machining of B< sub> 4</sub> C–TiB< sub> 2</sub> composites.* Journal of the European Ceramic Society, 2011. **31**(11): p. 2023-2030.
8. Anstis, G.R., et al., *A Critical Evaluation of Indentation Techniques for Measuring Fracture Toughness: I, Direct Crack Measurements.* Journal of the American Ceramic Society, 1981. **64**(9): p. 533-538.
9. Pasaribu, H.R., J.W. Sloetjes, and D.J. Schipper, *The transition of mild to severe wear of ceramics.* Wear, 2004. **256**(6): p. 585-591.
10. Metselaar, H., et al., *Wear of ceramics due to thermal stress: a thermal severity parameter.* Wear, 2001. **249**(10): p. 962-970.
11. Adachi, K., K. Kato, and N. Chen, *Wear map of ceramics.* Wear, 1997. **203**: p. 291-301.
12. Bos, J. and H. Moes, *Frictional heating of tribological contacts.* Journal of tribology, 1995. **117**(1): p. 171-177.
13. Hamilton, G.M., *Explicit equations for the stresses beneath a sliding spherical contact.* Proceedings of the Institution of Mechanical Engineers. Pt. C: Mechanical Engineering Science, 1983. **197**: p. 53-9.